MDPI

Hole Making by Electrical Discharge Machining (EDM) of γ-TiAl Intermetallic Alloys

Aitor Beranoagirre [1,*], **Gorka Urbikain** [1] (ID)**, Amaia Calleja** [2] (ID) **and**
Luis Norberto López de Lacalle [3] (ID)

[1]   Department of Mechanical Engineering, University of the Basque Country (UPV/EHU), Plaza Europa 1, 20018 San Sebastián, Spain; gorka.urbikain@ehu.eus

[2]   Department of Mechanical Engineering, University of the Basque Country (UPV/EHU), Nieves Cano 12, 01006 Vitoria, Spain; amaia.calleja@ehu.eus

[3]   CFAA, University of the Basque Country (UPV/EHU), Parque Tecnológico de Zamudio 202, 48170 Bilbao, Spain; norberto.lzlacalle@ehu.es

*   Correspondence: aitor.beranoagirre@ehu.eus; Tel.: +34-943-018-636

check for updates

Abstract: Due to their excellent strength-to-weight ratio and corrosion and wear resistance, γ-TiAl alloys are selected for aerospace and automotive applications. Since these materials are difficult to cut and machine by conventional methods, this study performed drilling tests using Electro Discharge Machining (EDM) to compare the machinability between two different types of γ-TiAl: extruded MoCusi and ingot MoCuSi. Different electrode materials and machining parameters were tested and wear, surface hardness, roughness and integrity were analyzed. The results indicate that extruded MoCuSi is preferable over MoCuSi ingots.

1. Introduction

Electrical discharge machining (EDM) is a widely used nontraditional machining process in industrial applications requiring high-profile accuracy and fine dimensional tolerances, especially when difficult-to-cut materials are involved. In particular, EDM drilling [1] is a commonly used process for orifice and hole machining in the aerospace, medical [2], molds and automotive sectors.

In an EDM process, the material is machined by electrical discharges. An electric arc is produced between the workpiece and the electrode until the desired shape is obtained. The workpiece and the electrode are submerged in a dielectric environment [3], both are also electrical conductors [4]. EDM is especially efficient for machining materials with high-hardness and complex geometries [5].

However, surface defects associated with EDM, such as voids, dense white layers, serious micro cracks and heat affected areas [6], require surface analysis [7] in order to guarantee machined component quality [8]. Moreover, electrode wear prediction and process parameter selection for process productivity, quality and accuracy requirements remain challenging with EDM.

In this sense, some authors study real-time monitoring techniques [9,10] in order to control electrode wear and to obtain an efficient EDM drilling process for nickel superalloys [11,12], titanium alloys [13–16], and stainless steel [17,18] workpieces.

Therefore, as it is often difficult to ensure the surface quality and the correct machining process, in this study, the results from EDM drilling tests in γ-TiAl are presented as a guide to ensure good surface quality and machining process performance. Within this context, different electrode materials and machining parameters were tested in order to determine optimal machining conditions. On this matter, electrode wear, surface hardness, roughness and integrity were analyzed and discussed. TiAl alloys are

widely used in areas such as aerospace, jet engines, airframe components and automotives due to their excellent corrosion resistance, lightweight and mechanical properties. Titanium and aluminum [19,20] are the most important components together with molybdenum (1–2%), copper and silicon (0.2%). They have very good thermal and mechanical properties such as: (1) low density (4 g/cm^3); (2) high temperature resistance; (3) excellent corrosion resistance and (4) good electric and thermal conductivity.

The literature regarding these materials is relatively scarce. Jabbaripour et al. [21] compared the powder mixed electrical discharge machining (PMEDM) and EDM process of γ-TiAl by changing the current, pulse on time, powder size and powder concentration. Shabgard et al. [22] used the EDM process for the machining of γ-TiAl and discussed the influence of the input parameters (discharge current and duration) on the removal rate, tool wear, or compositions and phases of machined surfaces. Holsten et al. [23] investigated the anomalous behavior of γ-TiAl, which is better machined under the conventional anodic polarity. This leads to TiC formation on the work surface.

In this work, EDM technology and process parameters are compared within two γ-TiAl types. Hole making operations using electrical discharges are made on extruded and ingot versions of this material for different machining regimes.

The MoCuSi TiAl alloy, depicted in Figure 1, is available in two versions: extruded or ingot. They are made from the same materials but differ in the way they are obtained. The former is obtained by casting, while the latter is obtained by extrusion performed in a stainless-steel sleeve. Due to this difference, the latter is covered in stainless steel.
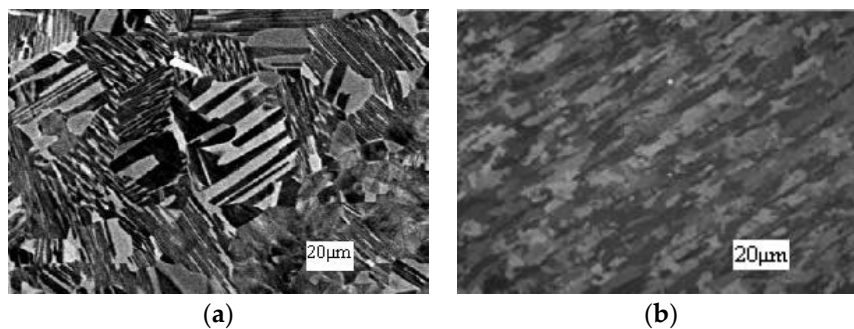
Figure 1. MoCuSi (**a**) ingot and (**b**) extruded. (courtesy of GfE® Metalle und Materialien GmbH).

Recently, TiAl alloys are a vast group with important differences between products. Table 1 shows the main differences between MoCuSi types and common Ti6Al4V. In the past, TiAl alloys were much easier to machine that the current TiAl alloys. As such, newer alloys have much lower density as well as higher maximum operating temperature. As both these properties are essential for current applications, this is a step forward for the industry.

**Table 1.** Properties of different TiAl alloys (courtesy of GfE® Metalle und Materialien GmbH).

Properties	MoCuSi Extruded	MoCuSi Ingot	Ti–6Al–4V (Annealed)
Density (g/cm^3)	3.74	3.88	4.49
Specific modulus (GPa/kg/m^3)	43	37	24
Tensile strength (MPa)	607	689	1087
Specific strength (MPa/(g/cm^3))	162	178	242
Yield strength (MPa)	589	570	942
Ductility (% elongation)	1.7	2.4	7.8
Fracture toughness (MPa·m$^{1/2}$)	23	20	52
Thermal conductivity (W/m/K)	24	19	8.6
Maximum operating temperature (°C)	900	865	615

Vacuum arc remelting (VAR), depicted in Figure 2a, is used in the manufacturing of ingots of γ-TiAl. The basic design of the VAR furnace has been continuously improved continuously, particularly

in regard to computer control and regulation, with the objective of achieving a fully-automated remelting process. This has resulted in improved reproducibility of the metallurgical properties of γ-TiAl ingots.

The process involves melting the material within a vacuum-controlled atmosphere (0.13–13 Pa) in order to develop material homogeneity. VAR is the continuous remelting of a consumable electrode by means of an arc under vacuum. Direct current (DC) power is applied to strike an arc between the consumable electrode (cathode −) and the baseplate of a copper mold contained in a water jacket (anode +). The intense heat generated by the electric arc melts the tip of the electrode and a new ingot is progressively formed in the water-cooled mold.

MoCuSi ingots are obtained by VAR while extruded MoCuSi is obtained by extruding MoCuSi ingots. This difference in processing results in substantial differences in properties, shown in Figure 2b. The extruded material [24–26] has more desirable properties than the ingots. Yield strength, creep strain and endurance limit are much lower in the ingots than in the extruded material. The difference in the fracture toughness is less pronounced.
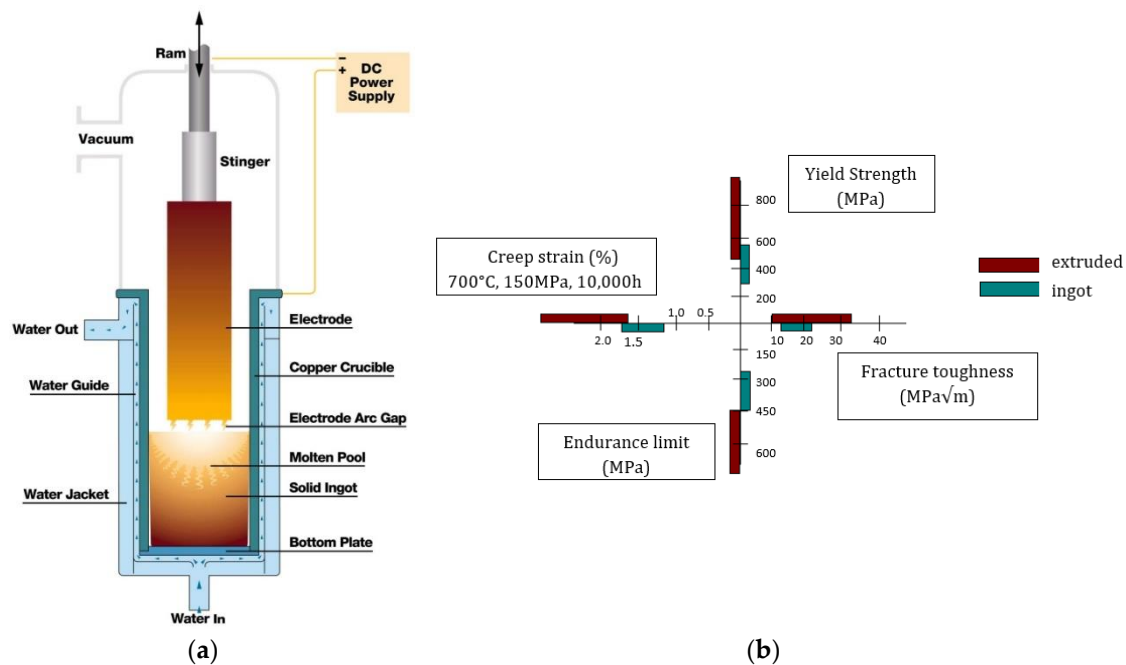
Figure 2. (**a**) Vacuum arc remelting (VAR) furnace (adapted from ATI Allvac©); (**b**) properties of extruded and ingot TiAl.

TiAl alloys are used for reliable components where surface integrity must be maintained. However, the machinability of titanium and its alloys is poor due to their low thermal conductivities, high chemical reactivity, and low elastic moduli, making it difficult to obtain good machining quality. To overcome these challenges, EDM could be an effective manufacturing process, especially for the manufacturing of complex geometries. In this process, a high temperature gradient can jeopardize process accuracy and the operating life of the part.

2. Experimental Procedure

γ-TiAl can be applied to a number of applications in the aerospace and automotive industries. This study was designed to determine the machinability and the best machining conditions for EDM of the extruded and ingot types of these titanium aluminides. The experimental procedure included the following steps: (1) experimental machining tests with different regimes, roughing and finishing,

using different strategies and parameters; (2) measurements of process quality: electrode wear, hole diameter, surface finish and hardness.

2.1. Machining Tests

For the EDM tests, a conventional EDM machine (ONA© Compact 2) was used, depicted in Table 2.

Table 2. ONA© Compact 2 characteristics.

	X-Y-Z axes travel	$350 \times 250 \times 380$ mm
	Machine dimensions	$1000 \times 750 \times 2000$ mm
	Worktable dimensions	550×360 mm
	Allowable weight on table	350 kg
	Generator intensity	30 A
	Voltage levels	9
	Electrode diameter	0.2–3 mm
	Water tank capacity	25 L

The next step was the design of the roughing and finishing operations for the ingot/extruded MoCuSi workpieces. Eight holes of 0.3 mm depth, four for roughing conditions and four for finishing operations, were made in both materials, shown in Figure 3. The number of attempts for roughing (four) and finishing (four) operations were chosen in order to adequately represent a number of cutting parameters within the machine's capabilities. Additionally, a 0.3 mm depth of cut was chosen to keep machining times reasonable as increasing this value leads to very long machining times.
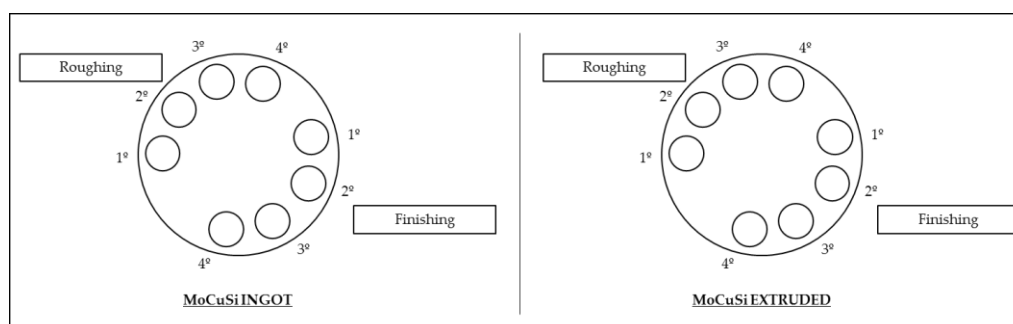
Figure 3. Scheme of electrical discharge machining (EDM) operations for both materials ordered by hole number.

In the EDM process, the electrode is one of the most important factors, accounting for around 60% of total process cost. Desirable electrode material properties are high fusion temperature, good conductivity, low expansion coefficient and low density. Regarding electrode material, in this case, graphite electrodes were used. The properties of these electrodes are shown in Table 3. Copper-tungsten electrodes were also tested, but these were discarded due to problems with erosion. Copper-tungsten electrodes required 1 h and 20 min for a 0.15 mm deep hole and it was impossible to obtain a deeper hole. Extra attempts were performed with higher machining values but this problem persisted. The main reason for such a failure is that copper-tungsten electrodes are not appropriate for titanium machining due to excessive electrode wear. Graphite's good thermal and electric properties and its machinability make it ideal for γ-TiAl machining. The most important property of graphite is related to state transformation: it does not pass from solid to liquid but passes directly from solid to gas, a process called sublimation.

Table 3. Properties of selected graphite electrodes (courtesy of *matweb©*).

Properties	Graphite
Density (kg/m^3)	1800
Particle size	1–5 μm
Bending resistance (kg/m^2)	5.3×10^6
Compression resistance (kg/m^2)	10.50×10^6
Hardness (HB)	70
Electrical resistivity (μΩ)	16

Test conditions (intensity, voltage, stages, impulse time (t_i) and pause time (t_o)) were established for both types of operations. Initially, the workpiece and electrode were placed in the right position, and the cleaning system was run. First, the roughing test was carried out and afterwards, the finishing test was performed. For the roughing test, the hole diameter was measured with a coordinate measuring machine (CMM) (Mitutoyo, Kawasaki, Kanagawa, Japan). Additionally, the electrode wear was studied by analyzing the height and weight losses. The lost height was measured by the wear electro discharge machine, it was measured before and after holes drilling. First of all, roughing tests were performed (more than 100 mm^3/min), testing different intensities, impulse and pause times. Roughing test conditions were selected depending on the gap, machining speed, and electrode wear.

The workpiece hardness changes during the EDM process due to the heat suffered by the electrode and the workpiece. Depending on the pulse time and the time between pulses, the workpiece suffers cooling and heating cycles. If the workpiece holds a temperature higher than the annealing temperature, hardening occurs. Therefore, after the EDM process, the hardness was measured in order to verify the influence of the machining parameters on surface hardness. This measurement was carried out at three different points in order to obtain reliable average results. For that purpose, a Mitutoyo© HR-300 (Mitutoyo, Kawasaki, Kanagawa, Japan) was used. The results of these experiments are shown in Table 3.

After machining the surface finish was measured with a Mitutoyo SJ-301 (Mitutoyo, Kawasaki, Kanagawa, Japan) with a measuring range of 12.5 mm. The results of these tests are shown in Table 4.

2.1.1. Roughing Tests

For roughing tests, shown in Tables 4 and 5, the power value was set to 100 V. The established polarity was negative for the electrode and positive for the piece. EDM parameters were programmed according to roughing conditions. However, pause times were increased due to the fluid lack of time for deionization. The pulse and pause times per period are represented by t_i and t_o respectively. The sum of t_i and t_o times gives the time period, which is the period between two consecutive sparks. The workpiece material being removed is represented by V_w. Black rectangles indicate critical regimes that could not be successfully tested during the experiments.

Table 4. Roughing parameters for the MoCuSi ingot.

Test	Intensity (A)				Stages Number	t_i (μs)	t_o (μs)	Lateral Gap (μm)	Removed Material Vol. V_w (mm^3/min)
1°	1	2	4	-	x 3	200	20	80	101
2°	1	2	4	8	x 2	200	20	120	170
3°	1	2	4	8	x 3	200	30	140	270
4°	1	2	4	8	x 4	200	30	150	330

In all the tests, the pause time, t_o, was increased for a more stable erosion. For the MoCuSi ingot workpiece, shown in Table 4, for the first and the second attempts, the pause time was increased from 6 μs to 20 μs, in the third attempt it was increased from 12 μs to 30 μs and in the fourth attempt it was increased from 6 μs to 30 μs. For the extruded MoCuSi, shown in Table 5, in the first, the third and the

fourth attempts the pause time was increased from 12 μs to 30 μs and in the second attempt it was increased from 12 μs to 20 μs.

Table 5. Roughing parameters for the extruded MoCuSi.

Test	Intensity (A)				Stages Number	t_i (μs)	t_o (μs)	Lateral Gap (μm)	Removed Material Vol. V_w (mm^3/min)
1°	1	2	4	-	x 3	200	30	80	101
2°	1	2	4	8	x 2	270	20	120	170
3°	1	2	4	8	x 3	200	30	140	270
4°	1	2	4	8	x 4	200	30	150	330

2.1.2. Finishing Tests

For finishing tests, the voltage used was 100 V, with positive polarity for the graphite electrode and negative polarity for the workpiece. For cases one and two for MoCuSi ingot component, shown in Table 6, were carried out with direct polarity, while for cases three and four, the polarity was inverted in order to decrease machining times.

Table 6. Finishing parameters for MoCuSi ingot.

Test	Intensity (A)				Stages Number	t_i (μs)	t_o (μs)	Ra (μm)	Type of Finish	Removed Material Vol. V_w (mm^3/min)
1°	1	2	-	-	x 1	16	6	1.6	N7	1.2
2°	1	2	-	-	x 2	50	6	3.2	N8	10
3°	1	2	-	-	x 4	200	12	6.3	N9	42
4°	1	-	-	-	x 2	150	6	12.6	N10	84

For extruded MoCuSi finishing tests, shown in Table 7, in the first, second and fourth attempts, the pause time (t_o) was increased from 6 μs to 12 μs for a more stable erosion. Moreover, two cleaning tubes were added for the fourth attempt for a better cleaning.

Table 7. Finishing parameters for the extruded MoCuSi.

Test	Intensity (A)				Stages Number	t_i (μs)	t_o (μs)	Ra (μm)	Type of Finish	Removed Material Vol. V_w (mm^3/min)
1°	1	2	-	-	x 1	16	12	1.6	N7	1.2
2°	1	2	-	-	x 2	50	12	3.2	N8	10
3°	1	2	-	-	x 4	200	12	6.3	N9	42
4°	1	-	-	-	x 2	150	12	12.6	N10	84

3. Results and Discussion

For ingot and extruded MoCuSi, the electrode wear, surface hardness, roughness and integrity were analyzed.

3.1. Electrode Wear

For MoCuSi ingots, shown in Table 8, the lateral gap of the first and fourth attempts was the smallest one. Moreover, the machining in the fourth attempt was 20 min faster. The diameter of the hole was measured three times using the CMM machine and the three measurements were averaged. The values were approximated to the nearest one in 0.01 mm even though the machine resolution was 0.001 mm. Table 7 shows that the values obtained in the first and fourth attempts were the closest to the nominal diameter of 18.5 mm. After further surface analysis, shown below, it was concluded that the holes in the first and fourth attempts had the best surface finish so the parameters of the fourth attempt were the most efficient of tested conditions.

Table 8. Roughing results for the ingot MoCuSi.

Hole	Test	Time	Weight (g)	Height Wear (mm)	Hole Diameter (mm)	Hole Diameter Average (mm)	Electrode Diameter (mm)	Lateral Gap (mm)
					Roughing MoCuSi Ingot			
Roughing 1	1 2 3	1 h 29 min	9.86	0.93	18.68 18.67 18.68	18.63		0.13
Roughing 2	1 2 3	1 h 3 min	9.38	0.76	18.68 18.67 18.67	18.65	18.50	0.15
Roughing 3	1 2 3	40 min	9.86	0.85	18.69 18.68 18.69	18.69		0.19
Roughing 4	1 2 3	1 h 8 min	8.64	0.91	18.67 18.66 18.65	18.63		0.13
Weight of the electrode at the beginning (g)							8.19	
Weight of the electrode at the end (g)							6.08	

For the extruded MoCuSi, shown in Table 9, the lateral gap in test #4 was the smallest one. The more intensity applied, the better the hole surface finish and precision obtained. In the following section, it was concluded that the electrode wear results obtained with the extruded MoCuSi workpiece are better as less time was required for hole machining for the same machining parameters.

Table 9. Roughing results for the extruded MoCuSi.

Hole	Attempt	Time	Weight (g)	Height Wear (mm)	Hole Diameter (mm)	Hole Diameter Average (mm)	Electrode Diameter (mm)	Lateral Gap (mm)
					Roughing MoCuSi Extruded			
Roughing 1	1 2 3	31 min	7.64	0.95	18.68 18.67 18.68	18.68		0.18
Roughing 2	1 2 3	1 h	7.08	0.90	18.68 18.67 18.67	18.67	18.50	0.17
Roughing 3	1 2 3	45 min	6.56	1.05	1869 18.68 18.69	18.69		0.19
Roughing 4	1 2 3	36 min	6.08	1.00	18.67 18.66 18.66	18.66		0.16
Weight of the electrode at the beginning (g)							8.19	
Weight of the electrode at the end (g)							6.08	

3.2. Hardness Results

The hardness measurements were made using a hardness testing machine HR-320MS (Mitutoyo, Kawasaki, Kanagawa, Japan). Three different hardness points were measurements in each hole surface. One was in the center of the hole and the other two were in the hole's vertical diameter 3 mm apart. Table 10 shows the obtained hardness values for ingot and extruded MoCuSi.

Table 10. Hardness with MoCuSi ingot/extruded roughing.

Measurement area	MoCuSi Ingot				MoCuSi Extruded			
	Tests				Tests			
	1	2	3	Average	1	2	3	Average
Without erosion	31.7	28.3	31.1	30.4	32	34.6	34.5	33.7
Finishing 1	30.4	29.8	32.6	30.9	34.7	32.3	34.9	34.0
Finishing 2	30.2	30.6	27.9	29.6	35.8	34.6	35.4	35.3
Finishing 3	27.9	30.8	31.7	30.1	36.4	35.4	35	35.6
Finishing 4	37.5	39.5	37.7	38.2	35.7	38.9	43.7	39.4
Roughing 1	26.2	24.4	29.8	26.8	45.3	41.5	26.5	37.8
Roughing 2	32.9	48.2	42.4	41.2	38.5	42.1	51.8	44.1
Roughing 3	54.6	46.7	49.2	50.2	39.7	52	59.8	50.5
Roughing 4	32	25.9	34.7	30.9	46.8	36	33.4	38.7

Figures 4 and 5 show that extruded MoCuSi presents always higher hardness values than the MoCuSi ingot in all the performed tests. For both materials, the hardness is relatively constant for low to moderate intensities. However, at high intensity values, the hardness is increased specially for the ingot type (x 1.3, from 30 to approx. 40 HB). The tendency is more accentuated for roughing operations where a hardness maximum is found for both materials at moderate intensities.
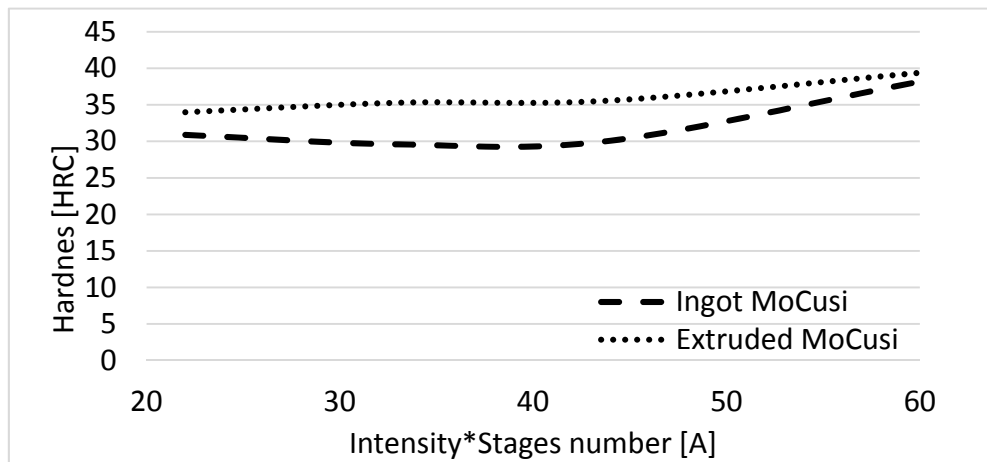

Figure 4. Comparison of hardness/intensity in finishing for both materials.
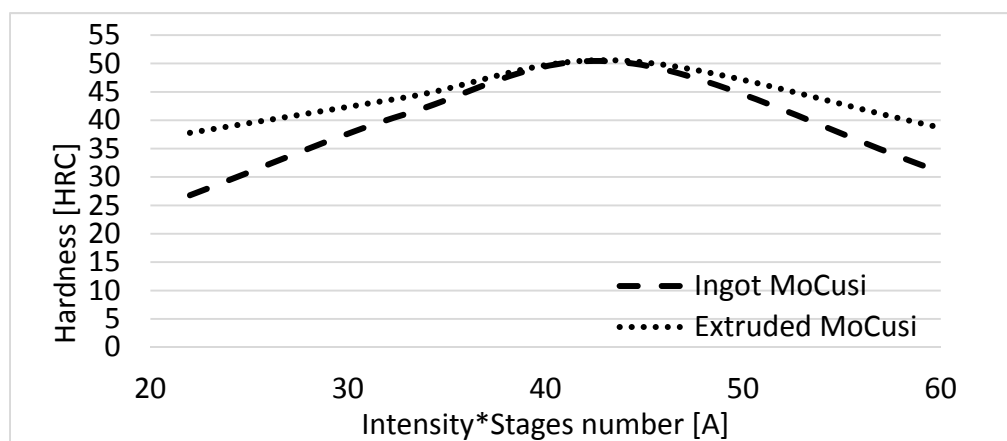
Figure 5. Comparison of hardness/intensity in roughing for both materials.

3.3. Roughness Results

Tables 11 and 12 show the roughness results for ingot and extruded MoCuSi respectively. As these tables show, the surface finish obtained was worse than in theoretical steel. In this case, in the first and second tests worse results in comparison to the finish of theoretical steel were obtained. On the contrary, in the third and fourth tests, similar results to the finish of theoretical steel were found.

Figure 6 shows the surface roughness evolution when increasing the removed material V_w. It demonstrates that extruded MoCuSi type always presents a better surface finish than ingot MoCuSi.

The following figures show the best and worst surface finish results for the finishing test for the ingot and extruded MoCuSi. The drilled surface and geometry edges were analyzed. Figure 7 shows MoCuSi ingot's best and worst surface finish. In this case, the best results correspond to the lowest machining volume. For higher machining volumes, the machined surfaced was damaged. Moreover, the best surface finish was obtained for the lowest intensity and impulse-time values.

Table 11. Results for surface finish with the ingot MoCuSi.

		Graphite Electrode and MoCuSi Ingot Piece			
Test	**Ra (μm)**	**Rz (μm)**	**Rt (μm)**	**Finish Type**	**Theoretical Steel Finish**
1°	2.654	16.682	23.676	N8	N7
2°	4.583	24.999	34.282	N9	N8
3°	6.443	36.948	45.181	N10	N9
4°	13.165	79.028	116.375	N11	N10
		Length			4.8 mm

Table 12. Results for surface finish with the extruded MoCuSi.

		Graphite and MoCuSi Extruded Piece			
Test	**Ra (μm)**	**Rz (μm)**	**Rt (μm)**	**Finish Type**	**Theoretical Steel Finish**
1°	2.786	18.554	20.605	N8	N7
2°	6.989	40.692	49.935	N10	N8
3°	5.030	32.020	45.207	N9	N9
4°	10.533	55.518	71.361	N10	N10
		Length			4.8 mm
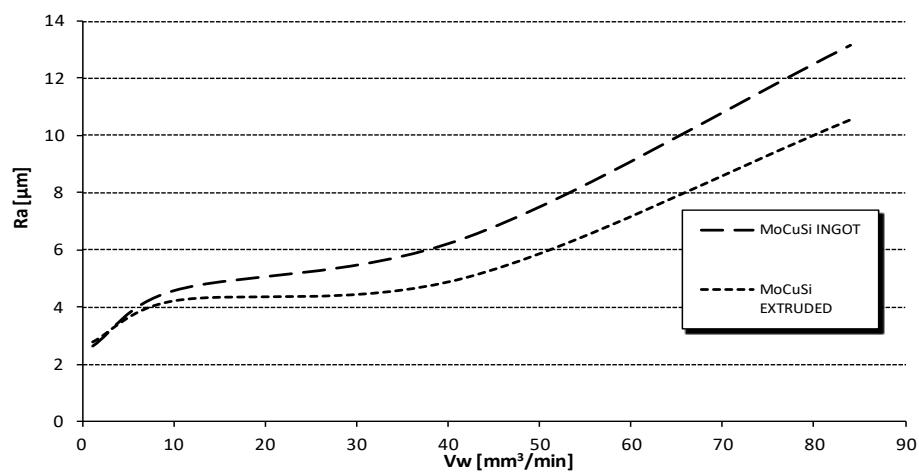
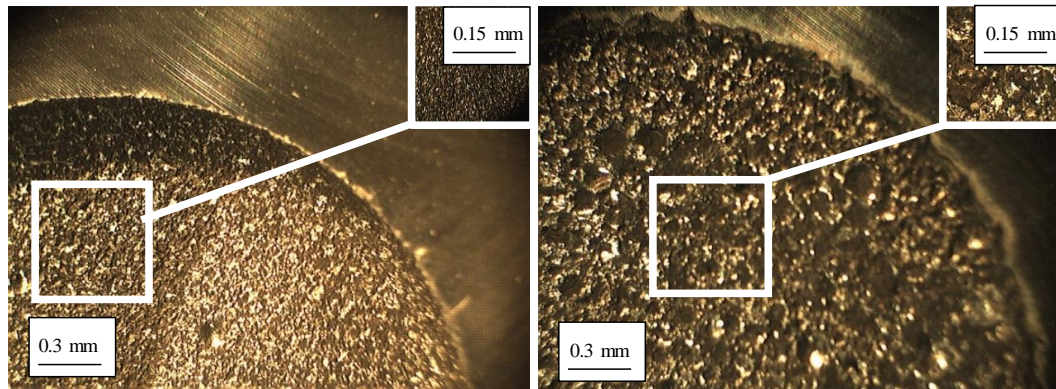**Figure 6.** Surface finish and machining volume for the ingot and extruded MoCuSi.
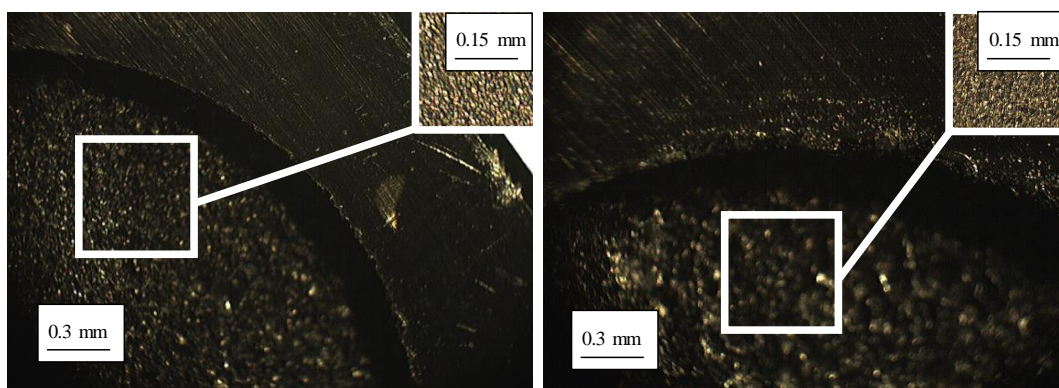
Figure 7. Details of the best (**left**) and worst (**right**) edge and surface finish with the MoCuSi ingot.

Figure 8 shows the best and worst edge and surface finish for extruded MoCuSi. Similar to the ingot MoCuSi, the best surface finish results were obtained with the lowest machining volumes

tested. Tested high machining volumes led to damaged surfaces. Moreover, the best surface finish was obtained for low intensity and pulse-time values.

Regarding surface integrity, it can be concluded that ingot and extruded MoCuSi present similar behavior for the same machining conditions, but extruded MoCuSi presents a better surface finish.


Figure 8. Details of the best (**left**) and worst (**right**) edge and surface finish with the MoCuSi ingot.

Due to the erosion and the corrosion (chemical and thermal attack), the electrodes suffer wear. Figure 9 shows the difference between electrode surface at the beginning of the machining process and once the machining process was finished. As shown in the figure, the graphite surface suffers wear during the machining process.
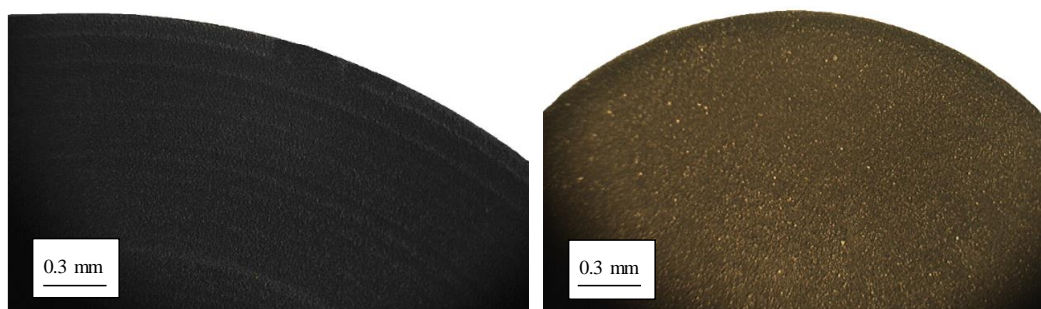
Figure 9. The difference between the graphite electrode before and after being used.

Figure 10 shows the wear suffered by the electrode profile. The angle of the electrode was 90° at the beginning and is subsequently reduced due to the suffered damage.
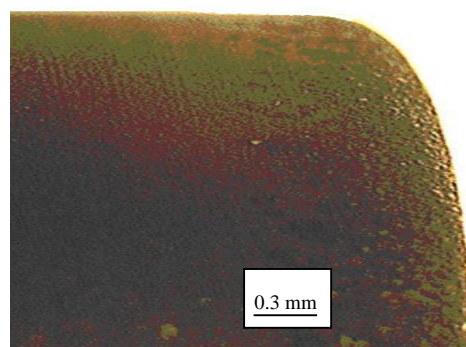
Figure 10. The profile of the graphite electrode after being used.

4. Conclusions

γ-TiAl alloys possess better mechanical properties than classical TiAl alloys and so, there is a chance to substitute the latter with the former. However, the lower machinability of γ-TiAl alloys is an obstacle that needs to be addressed. In this study, the machinability of two types of γ-TiAl alloys, ingot MoCuSi and extruded MoCuSi, was compared.

After material analysis, it can be concluded that, in general, MoCuSi alloys present a similar behavior.

Considering the surface finish, both MoCuSi alloys present a similar behavior. The best results are obtained with the extruded MoCuSi workpiece but, in general, the difference between both is subtle.

Moreover, in roughing tests, the best results were also obtained with extruded MoCuSi: the lowest times and the best surface finish results. In the roughing test, tested parameters on the first and the fourth attempts present the best surface finish results. For the fourth attempt, the machining time was shorter than the first one. In relation to this, intensity and stage number influence was observed: higher intensity values determine shorter machining times.

In relation to hardness analysis, the extruded MoCuSi workpiece presents harder values than the MoCuSi ingot. In general, after roughing tests, higher hardness values were measured than after finishing tests. Thus, the extruded type is more preferable than the MoCusi ingot due to its superior mechanical properties.

On the other hand, regarding electrode materials, although both graphite and copper-tungsten electrodes were tested, copper-tungsten electrodes were found to be inappropriate for titanium component machining due to unstable erosion and excessive electrode wear. For that reason, graphite electrodes were used for this study.

Author Contributions: A.B. designed and performed the experiments. G.U. and A.C. analyzed roughness, hardness, electrode wear and surface integrity. Finally, L.N.L.d.L. contributed with the resources (machine, tools, material, etc.) and general supervision of the work.

References

1. Bellotti, M.; Qian, J.; Reynaerts, D. Enhancement of the Micro-EDM Process for Drilling Through-holes. *Proced. CIRP* **2018**, *68*, 610–615. [CrossRef]
2. Ho, K.H.; Newman, S.T. State of the art electrical discharge machining (EDM). *Int. J. Mach. Tools Manuf.* **2003**, *43*, 1287–1300. [CrossRef]
3. Bojorquez, B.; Marloth, R.T.; Es-Said, O.S. Formation of a crater in the work piece on an electrical discharge machine. *Eng. Fail. Anal.* **2002**, *9*, 93–97. [CrossRef]
4. Marafona, J.; Chousal, J.A.G. A finite element model of EDM based on the Joule effect. *Int. J. Mach. Tools Manuf.* **2005**, *46*, 1–8. [CrossRef]
5. Mai, C.; Hocheng, H.; Huang, S. Advantages of carbon nanotubes in electrical dis-charge machining. *Int. J. Adv. Manuf. Technol.* **2012**, *59*, 111–117. [CrossRef]
6. Tzeng, Y.F.; Lee, C.Y. Effects of powder characteristics on electrodischarge machining efficiency. *Int. J. Adv. Manuf. Technol.* **2001**, *17*, 586–592. [CrossRef]
7. Mohammadreza, S.; Behnam, K. Investigation of carbon nanotube added dielectric on the surface characteristics and machining performance of Ti–6Al–4V alloy in EDM process. *J. Manuf. Process.* **2017**, *25*, 212–219. [CrossRef]

8. Hsu, W.-H.; Chien, W.-T. Effect of Electrical Discharge Machining on Stress Concentration in Titanium Alloy Holes. *Materials* **2016**, *9*, 957. [CrossRef] [PubMed]

9. Nirala, C.K.; Saha, P. Precise μEDM-drilling using real-time indirect tool wear compensation. *J. Mater. Process. Technol.* **2017**, *240*, 176–189. [CrossRef]

10. Aligiri, E.; Yeo, S.; Tan, P. A new tool wear compensation method based on real-time estimation of material removal volume in micro-EDM. *J. Mater. Process. Technol.* **2010**, *210*, 2292–2303. [CrossRef]

11. Kliuev, M.; Boccadoro, M.; Perez, R.; Dal Bó, W.; Stirnimann, J.; Kuster, F.; Wegener, K. EDM Drilling and Shaping of Cooling Holes in Inconel 718 Turbine Blades. *Proced. CIRP* **2016**, *42*, 322–327. [CrossRef]

12. Torres, A.; Puertas, I.; Luis, C.J. EDM machinability and surface roughness analysis of INCONEL 600 using graphite electrodes. *Int. J. Adv. Manuf. Technol.* **2016**, *84*, 2671–2688. [CrossRef]

13. Yilmaz, O.; Okka, M.A. Effect of single and multi-channel electrodes application on EDM fast hole drilling performance. *Int. J. Adv. Manuf. Technol.* **2010**, *51*, 185–194. [CrossRef]

14. Yadav, U.S.; Yadava, V. Experimental Investigation on Electrical Discharge Drilling of Ti-6Al-4V Alloy. *Mach. Sci. Technol.* **2015**, *19*, 515–535. [CrossRef]

15. Lin, M.Y.; Tsao, C.C.; Huang, H.H.; Wu, C.Y.; Hsu, C.Y. Use of the grey Taguchi method to optimise the micro-electrical discharge machining (micro-EDM) of Ti-6Al-4V alloy. *Int. J. Comput. Integr. Manuf.* **2014**, *28*, 569–576. [CrossRef]

16. Meena, V.K.; Azad, M.S. Grey Relational Analysis of Micro-EDM Machining of Ti-6Al-4V Alloy. *Mater. Manuf. Process.* **2012**, *27*, 973–977. [CrossRef]

17. Rashed, C.A.A.; Romoli, L.; Tantussi, F.; Fuso, F.; Bertoncini, L.; Fiaschi, M.; Allegrini, M.; Dini, G. Experimental optimization of micro-electrical discharge drilling process from the perspective of inner surface enhancement measured by shear-force microscopy. *CIRP J. Manuf. Sci. Technol.* **2014**, *7*, 11–19. [CrossRef]

18. D'Urso, G.; Maccarini, G.; Quarto, M.; Ravasio, C. Investigation on power discharge in micro-EDM stainless steel drilling using different electrodes. *J. Mech. Sci. Technol.* **2015**, *29*, 4341–4349. [CrossRef]

19. López de Lacalle, L.N.; Lamikiz, A. *Machine Tools for High Performace Machining*, 1st ed.; Springer: London, UK, 2009; ISBN 978-1848003798.

20. Sharman, A.R.C.; Aspinwall, D.K.; Dewes, R.C.; Bowen, P. Workpiece surface integrity considerations when finish turning gamma titanium aluminide. *Wear* **2001**, *249*, 473–481. [CrossRef]

21. Jabbaripour, B.; Sadeghi, M.H.; Shabgard, M.R. Investigating surface roughness, material removal rate and corrosion resistance in PMEDM of γ-TiAl intermetallic. *J. Manuf. Process.* **2013**, *15*, 56–68. [CrossRef]

22. Shabgard, M.; Faraji, H.; Khosrozadeh, B.; Amini, K.; Seyedzavvar, M. Experimental investigation into the EDM process of gamma-TiAl. *Turk. J. Eng. Environ. Sci.* **2014**, *38*, 231–239. [CrossRef]

23. Holsten, M.; Koshy, P.; Klink, A.; Schwedt, A. Anomalous influence of polarity in sink EDM of titanium alloys. *CIRP Ann.* **2018**, in press. [CrossRef]

24. Olvera, D.; Urbikain, G.; Beranoagirre, A.; López de Lacalle, L.N. *Hole Making in Gamma TiAl*, 1st ed.; DAAAM International Publications: Wien, Austria, 2010; pp. 337–347. ISBN 978-3-901509-86-5.

25. Beranoagirre, A.; Olvera, D.; López de Lacalle, L.N.; Urbicain, G. Drilling of Intermetallic Alloys Gamma TiAl. *AIP Conf. Proc.* **2011**, *1315*, 1023–1028.

26. Lee, P.; Altintas, Y. Prediction of ball-end milling forces from orthogonal cutting data. *Int. J. Mach. Tools Manuf.* **1996**, *36*, 1059–1072. [CrossRef]